

# Coupled two-component atomic gas in an optical lattice

Jonas Larson and Jani-Petri Martikainen

*NORDITA, 106 91 Stockholm, Sweden*

(Dated: February 13, 2019)

We study the ground state of an ideal coupled two-component gas of ultracold atoms in a one dimensional optical lattice, either bosons or fermions. Due to the internal two-level structure of the atoms, the Brillouin zone is twice as large as imposed by the periodicity of the lattice potential. This is reflected in the Bloch dispersion curves, where the energy bands regularly possess several local minima. As a consequence, when the system parameters are tuned across a resonance condition, a non-zero temperature topological first order phase transition occurs which arises from an interplay between internal and kinetic atomic energies. It is shown that these phenomena are also captured for two and three dimensional optical lattices.

PACS numbers: 37.10.Jk,05.30.Jp,05.30.Fk,03.75.Mn

## I. INTRODUCTION

The coupled dynamics between an ultracold atomic gas and an optical lattice has gained enormous attention during the last decade. Originally, D. Jaksch *et al.* proposed that the *Mott-superfluid* quantum phase transition (PT) can be realized using cold atoms dipole coupled to a standing wave laser field [1]. A mere four years later, this PT was observed in the seminal experiment by I. Bloch and coworkers [2]. One among the many reasons for the great interest in these systems is the possibility to experimentally realize, and therefore verify, theoretical models developed in the field of condensed matter physics, see the review [3]. Several achievements in this field have been accomplished both theoretically and experimentally, and to only mention a few; disordered systems and matter localization [4], frustrated systems [5], the strong atom-atom interaction regime and the Tonks gas [6], cold atom quantum Hall counterparts [7] and quantum information processing [8].

Almost exclusively, effective dispersive models have been considered, where the internal level structure of the atoms can be discarded and one is left with a single atomic level. Exceptions are works on spin-dependent atoms, which have shown to acquire new phases compared to the spinless case [9]. Another, related system is mixtures of different atomic species, again containing novel physics [10]. However, these models do not analyze direct coupling between the internal atomic states, as will be the topic of the present paper. Furthermore, atom-atom scattering plays a crucial role in the dynamics of all above references. For example, the Mott-superfluid PT in the *Bose-Hubbard model* arises from a competition between the atomic kinetic energy (hopping between neighboring sites) and the onsite scattering interaction [11]. Here we will show that by taking into account for dipole induced transitions between coupled atomic states, PTs can occur even for ideal gases lacking atom-atom interaction. This originates from the competition between the atomic kinetic and the internal energies, in comparison with kinetic and scattering energies.

We do not restrict the character of the atom-field inter-

action to be dispersive. In fact, we allow for a vanishing atom-field detuning and in particular study the behavior for both positive and negative detunings. Coupling between internal levels of atoms in optical lattices is rather unexplored. To the best of our knowledge, this has only been analyzed by Kuritsky *et al.* where they considered effective coupled two or three level models derived from RAMAN interactions [12, 13]. They found that the hopping term in the corresponding Bose-Hubbard model may be tuned to be either positive or negative, leading to new phases. Contrary to [12, 13], we consider here a direct coupling between two atomic levels, which is actually what one gets in the standard optical lattice model by decreasing the amplitude of the detuning. The detuning in our model may be seen as having similar role as the parameter  $\theta$  (relative phase between the two RAMAN lasers) in [12]. We show that the two-level structure of our model renders dispersion curves having local minima. It is known that such phenomena can give rise to topological PTs [14, 15, 16], which indeed are found in our model as well. Both for fermions and bosons, a topological PT does take place when the detuning changes sign. The non-zero temperature situation is also considered and the topological PT is found to be stable against temperature fluctuations.

The outline of this paper is as follows. We first discuss the single particle Hamiltonian in Sec. II, and point out some of the symmetries associated with it. One of these symmetry operators indicates that the Brillouin zone extends over twice the size expected from the periodicity of the optical lattice, a fact that is clarified even further in the proceeding Sec. III. In Sec. III we begin by analyzing the energy spectrum and the two lowest bands' Wannier functions. Using this knowledge we demonstrate the presence of a topological PT, both for fermions and bosons at zero and non-zero temperatures. A discussion of possible extensions is left for the conclusions given in IV. Finally, in the appendix IV we also present an effective RAMAN coupled model that would provide the same results, but with the benefit of using two metastable atomic states.

## II. SINGLE PARTICLE HAMILTONIAN

The Hamiltonian for a single two-level atom, whose internal states dipole couple via a standing wave laser field, reads

$$\hat{H} = \frac{\hat{p}^2}{2m} + \frac{\hbar\tilde{\Delta}}{2}\hat{\sigma}_z + 2\hbar\tilde{g}\cos(k\hat{x})\hat{\sigma}_x. \quad (1)$$

Here,  $\hat{p}$  and  $\hat{x}$  are atomic center-of-mass momentum and position,  $m$  its mass,  $\tilde{\Delta}$  the atom-field detuning,  $\tilde{g}$  the effective atom-field coupling and  $\tilde{k}$  the field wave number. The internal states of the atom are labeled  $|\pm\rangle$  and the Pauli matrices operates as  $\hat{\sigma}_z|\pm\rangle = \pm|\pm\rangle$  and  $\hat{\sigma}_x|\pm\rangle = |\mp\rangle$ . Before proceeding we introduce dimensionless variables through the characteristic length  $k^{-1}$  and energy  $E_r = \hbar^2 k^2 / 2m$ ;

$$\hat{x} = k\hat{x}, \quad \Delta = \frac{\hbar\tilde{\Delta}}{E_r}, \quad g = \frac{\hbar\tilde{g}}{E_r}. \quad (2)$$

In the  $|+\rangle = \begin{bmatrix} 1 \\ 0 \end{bmatrix}$  and  $|-\rangle = \begin{bmatrix} 0 \\ 1 \end{bmatrix}$  nomenclature, Eq. (1) becomes in scaled variables

$$\hat{H} = -\frac{\partial^2}{\partial x^2} + \begin{bmatrix} \frac{\Delta}{2} & 2g\cos(\hat{x}) \\ 2g\cos(\hat{x}) & -\frac{\Delta}{2} \end{bmatrix}, \quad (3)$$

which serves as our model Hamiltonian. We note that the external field couples the *bare states*  $|\pm\rangle$  and simultaneously shift the momentum by either  $\pm 1$ . For  $\Delta = 0$ , the unitary operator  $\hat{U} = \frac{1}{\sqrt{2}}(\hat{\sigma}_x + \hat{\sigma}_z)$  decouples the internal levels, and one obtains two Mathieu equations [17] with *adiabatic potentials*  $V_{\pm}^d(x) = \pm 2g\cos(x)$  [18]. The internal atomic states of the decoupled equations are

$$\begin{aligned} |1\rangle &= \hat{U}|+\rangle = \frac{1}{\sqrt{2}}(|+\rangle + |-\rangle), \\ |2\rangle &= \hat{U}|-\rangle = \frac{1}{\sqrt{2}}(|+\rangle - |-\rangle). \end{aligned} \quad (4)$$

For any parameters, the operator  $\hat{T} = e^{i\lambda\hat{p}}$  commutes with the Hamiltonian, where  $\lambda = 2\pi/k$  is the field wave length. Not as evident, is that also the operator

$$\hat{I} = \hat{\sigma}_z e^{i\frac{\lambda}{2}\hat{p}} \quad (5)$$

is a symmetry of the Hamiltonian [19, 20]. Thus, there is a natural  $\lambda/2$  periodic structure of the Hamiltonian. This signals that the first Brillouin zone ranges between  $-1$  and  $1$ , rather than  $-1/2 < q \leq 1/2$  as implied by the  $\lambda$  periodicity of the  $\hat{T}$  operator. However, for  $\Delta = 0$  the spectrum is doubly degenerate and in this limit it might be more convenient to define the Brillouin zone within  $-1/2 < q \leq 1/2$ . One may note that  $\hat{T} = \hat{I}^2$ . The physical background of this additional symmetry operator  $\hat{I}$  emerges from the fact that absorption or emission of a single photon flips the internal states,  $|\pm\rangle \rightarrow |\mp\rangle$ , while only for a two-photon process is the internal state unchanged.

## III. STRUCTURE OF THE GROUND STATE

### A. Model characteristics

To find the ground state of  $N$  non-interacting two-level atoms we need to diagonalize (3); within both the internal and the motional degrees of freedom. We first note that for a given quasi momentum  $q$ , the Hamiltonian can be written on the block form  $H = H_\varphi \otimes H_\phi$ , and the states coupled by the sub-Hamiltonians read

$$\begin{aligned} |\varphi_\eta(q)\rangle &= \begin{cases} |q+\eta\rangle|-\rangle & \eta \text{ even} \\ |q+\eta\rangle|+\rangle & \eta \text{ odd} \end{cases} \\ |\phi_\eta(q)\rangle &= \begin{cases} |q+\eta\rangle|+\rangle & \eta \text{ even} \\ |q+\eta\rangle|-\rangle & \eta \text{ odd}, \end{cases} \end{aligned} \quad (6)$$

where the first ket is the momentum eigenstate  $\hat{p}|q+\eta\rangle = (q+\eta)|q+\eta\rangle$  and  $\eta$  is an integer corresponding to the momentum shift governed by absorption and emission of photons. This decoupling of the dynamics is of great importance as a given number of atoms residing in each subset is constant when the parameters are varied. The states (6) are eigenstates of the Hamiltonian in the absence of matter-field coupling  $g = 0$ , with *bare energies*

$$\varepsilon^\mu = (q+\eta)^2 \pm (-1)^\mu \frac{\Delta}{2}, \quad (7)$$

where the  $\pm$ -sign is different for the two sets (6). In this trivial situation, the detuning  $\Delta$  simply shifts the parabolic dispersions. The general eigenstate, *Bloch state*, is characterized by a quasi momentum  $q$  and a band index  $\nu = 1, 2, 3, \dots$

$$\hat{H}|\psi_\nu(q)\rangle = E^\nu(q)|\psi_\nu(q)\rangle. \quad (8)$$

Here,  $E^\nu(q)$  is the  $\nu$ 'th energy band/dispersion curve. The eigenstate in a position representation can be written using its *constituent Bloch states* as

$$\begin{aligned} \psi_{\nu,q}(x) &= \langle x|\psi_\nu(q)\rangle = \psi_{\nu,q}^+(x)|+\rangle + \psi_{\nu,q}^-(x)|-\rangle \\ &= \psi_{\nu,q}^1(x)|1\rangle + \psi_{\nu,q}^2(x)|2\rangle. \end{aligned} \quad (9)$$

Note that the above specifies just two different constituent Bloch states and any other internal basis would define two new ones. In particular,  $\psi_{\nu,q}^{1,2}(x)$  and  $\psi_{\nu,q}^\pm(x)$  are related via the operator  $\hat{U} = \frac{1}{\sqrt{2}}(\hat{\sigma}_x + \hat{\sigma}_z)$  of Eq. (4). In terms of the the dispersions, the Hamiltonian is given by

$$\hat{H} = \sum_{\nu=1}^{\infty} \sum_{q \in (-1,1]} [E^\nu(q) - \mu] \hat{n}_q^\nu, \quad (10)$$

where  $\hat{n}_q^\nu$  is the operator giving the number of atoms with energy  $E^\nu(q)$  and here we have introduced a chemical potential  $\mu$ . Note that for a given atom number  $N$  one has  $\sum_{\nu=1}^{\infty} \sum_{q \in (-1,1]} \langle \hat{n}_q^\nu \rangle = N$ , where  $\langle \hat{n}_q^\nu \rangle$  is the expectation

value for the particular state of interest. The Bloch states can be expressed in the *bare basis* (6)

$$|\psi_\nu(q)\rangle = \begin{cases} \sum_{\eta=-\infty}^{\infty} c_\eta^\nu(q)|\varphi_\eta(q)\rangle \\ \sum_{\eta=-\infty}^{\infty} d_\eta^\nu(q)|\phi_\eta(q)\rangle \end{cases}. \quad (11)$$

Note that expanding  $|\psi_\nu(q)\rangle$  does not mix the states  $|\varphi_\eta(q)\rangle$  and  $|\phi_\eta(q)\rangle$  due to the block-diagonal form of the Hamiltonian  $H = H_\varphi \otimes H_\phi$  in this bare basis. We emphasize that a quasi momentum eigenstate, or Bloch state, is a linear combination of the two internal atomic states  $|\pm\rangle$ . The same holds for the Wannier functions

$$\begin{aligned} w_\nu(x-R) &\equiv \sum_{q \in (-1,1]} e^{iqR} \psi_{\nu,q}(x) \\ &= w_\nu^+(x-R)|+\rangle + w_\nu^-(x-R)|-\rangle \\ &= w_\nu^1(x-R)|1\rangle + w_\nu^2(x-R)|2\rangle. \end{aligned} \quad (12)$$

As defined above, the *constituent Wannier functions*  $w_\nu^+(x-R)$  and  $w_\nu^-(x-R)$  are normalized as  $\sum_{i=\pm} \int |w_\nu^i(x-R)|^2 dx = 1$ , and likewise for  $w_\nu^1(x-R)$  and  $w_\nu^2(x-R)$ . Like for the Bloch states, the constituent parts depend on the internal basis. Equipped with this machinery, we now turn to analyze the complex band structure of the Hamiltonian (3).

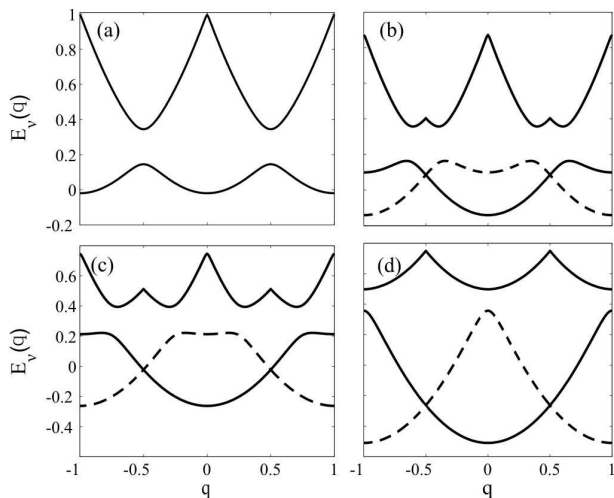


FIG. 1: The three lowest energy bands of Hamiltonian (3), where the scaled dimensionless parameters are  $g = 0.1$  and  $\Delta = 0, 0.25, 0.5, 1$  in plots (a)-(d) respectively. The two lowest bands are distinguished between the two sub-Hamiltonians  $H_\varphi$  (solid line) and  $H_\phi$  (dashed line).

Figure 1 displays some examples of the band structure and the dispersion curves, where the first three bands are shown. The resonance case,  $\Delta = 0$ , is given in (a) and

here the energy spectrum is doubly degenerate as pointed out in the previous section. However, for non-zero  $\Delta$ , the degeneracy is lifted (indicated in (b)-(d)) and as a consequence, the first Brillouin zone extends over quasi momenta  $q \in (-1, 1]$ . The dashed line corresponds to the lowest dispersion curve of the sub-Hamiltonian  $H_\phi$ , while the other lowest line derives from  $H_\varphi$  instead. Note that the dispersion curves have more than a single minimum in all plots. The non monotonicity of the dispersion curves can be understood from the interplay between the different energies; kinetic energy causing the parabolic structures, the coupling energy which typically splits the degeneracy and the internal atomic energy that (loosely speaking) shifts the dispersions.

Let us briefly discuss the dispersion curves and their limiting cases in more detail. In the regular dispersive situation one has  $\Delta \gg g$  and the coupling between the internal adiabatic states can be neglected. To verify this, let us introduce the *adiabatic states* [21] as columns of the unitary operator

$$\hat{U}_{ad} = \begin{bmatrix} \cos(\theta/2) & \sin(\theta/2) \\ \sin(\theta/2) & -\cos(\theta/2) \end{bmatrix}, \quad (13)$$

where

$$\tan(\theta) = \frac{4g \cos(x)}{\Delta}. \quad (14)$$

The operator  $\hat{U}_{ad}$  then diagonalizes the  $2 \times 2$  matrix of the Hamiltonian (3). However, due to its  $x$ -dependence will it not commute with the momentum operator  $\hat{p}$ . This causes non-diagonal terms in the transformed Hamiltonian [21],

$$\begin{aligned} \tilde{H} &= \hat{U} \hat{H} \hat{U}^{-1} = -\frac{\partial^2}{\partial x^2} + V_{cent}(\hat{x}) \\ &+ \begin{bmatrix} V_+^{ad}(\hat{x}) & \Omega(\hat{x}, \hat{p}) \\ \Omega^*(\hat{x}, \hat{p}) & V_-^{ad}(\hat{x}) \end{bmatrix}. \end{aligned} \quad (15)$$

Here,  $V_{cent}(x)$  is a *centrifugal* term turning up on the diagonal [22],  $\Omega(x, p)$  is the *non-adiabatic coupling* [21] and specifically

$$V_\pm^{ad}(x) = \pm \sqrt{\left(\frac{\Delta}{2}\right)^2 + 4g^2 \cos^2(x)} \quad (16)$$

are the *adiabatic potentials*. It follows that the centrifugal and adiabatic correction terms are small in the  $\Delta \gg g$  regime [21], giving the adiabatic potentials

$$V_\pm^{ad}(x) \approx \pm \frac{\Delta}{2} \pm \frac{4g^2 \cos^2(x)}{\Delta}. \quad (17)$$

Thus, we derive the regular situation most commonly considered in the literature and we especially note that the first Brillouin zone extends over  $q \in (-1, 1]$ . Choosing  $\Delta > 0$  and consider the weak coupling limit  $4g^2/\Delta \rightarrow 0$ , the states  $|q\rangle|-\rangle$  with  $q \in (-1, 1]$  have eigenvalues

$$E^0(q) = \varepsilon^0 = q^2 - \frac{\Delta}{2}. \quad (18)$$

For the states  $|q \pm 1\rangle|-\rangle$  on the other hand, we have the dispersions

$$E^0(q) = (q \pm 1)^2 - \frac{\Delta}{2}. \quad (19)$$

However, noticeable from Eq. (6), the states  $|q\rangle|-\rangle$  and  $|q \pm 1\rangle|-\rangle$  are not coupled and one restricts the analysis to just one of these sets and consequently regains a regular spectrum, by which we mean that the dispersion curves possess only a single minimum within one Brillouin length,  $dE^1(q)/dq \geq 0$  for  $0 \leq q \leq 1$ . More interesting is the intermediate regime, neither adiabatic nor *diabatic* ( $\Delta = 0$ ), where the above states may indeed coexist if we assume that both of the states  $|q\rangle|\pm\rangle$  can be present. Thus, when the coupling between  $|\pm\rangle$  states cannot be neglected, one must take into account all the states and the lowest energy band contains minima at  $q = \pm 1$  as well as for  $q = 0$ . As pointed out, here we allow for atomic states  $|+\rangle$  and  $|-\rangle$  to have the same momentum. It is understood that the same arguments hold for  $\Delta < 0$ , making the replacement  $|+\rangle \leftrightarrow |-\rangle$ . We should mention that even if we only consider atoms within one subset (6), the dispersion curves will contain several local minima [20, 23], and the results presented are valid also in such cases. In the diabatic limit,  $\Delta = 0$ , we saw that we can separate the dynamics into two uncoupled problems with *diabatic potentials*  $V_{\pm}^d(x) = \pm 2g \cos(x)$ . The spectrum is then doubly degenerate and the first Brillouin zone is therefore most properly defined within  $q \in (-1/2, 1/2]$ . Noteworthy is the fact that the diabatic potentials have minima either for  $x_m^{d-} = 2n\pi$  or  $x_m^{d+} = (2n+1)\pi$  for integer  $n$ , while the minima for the adiabatic potentials are either  $x_m^{a-} = n\pi$  or  $x_m^{a+} = (n + \frac{1}{2})\pi$ . By the  $\pm$ -sign we indicate the corresponding diabatic or adiabatic potential.

The coupled two-level character of the system gives rise to rather peculiar constituent Wannier functions  $w_{\nu}^{\pm}(x-R)$  or  $w_{\nu}^{1,2}(x-R)$ . In general,  $R$  is chosen such that the potential is minimal at  $x = R$ . However, in the present model  $R$  is not *a priori* given since the potential has a complex two-level structure. From the symmetry of the Hamiltonian it follows that  $w_{\nu}^{+}(x-R) \leftrightarrow w_{\nu}^{-}(x-R)$  for  $\Delta \leftrightarrow -\Delta$ , while  $|w_{\nu}^{1,2}(x-R)|$  are invariant under such sign change. In Fig. 2 (a)-(d) we show examples of  $|w_1^{\pm}(x-R)|^2$  (a) and (b) and  $|w_2^{\pm}(x-R)|^2$  (c) and (d), for  $R = 0$  or  $R = \pi/2$ . The dashed line shows  $|w_1^{-}(x-R)|^2$  and the solid  $|w_1^{+}(x-R)|^2$ . Note that for  $R = 0$ , the two constituent Wannier functions identical, which, however, does not hold for  $R = \pi/2$ . For  $R = 0$ , the constituent Wannier functions resemble typical ones obtained in one component systems [24]. This is not true for  $R = \pi/2$  (corresponding to the minima of  $V_{\pm}^{ad}(x)$ ), where only  $|w_{\nu}^{-}(x-R)|^2$  shows the regular shape and  $|w_1^{+}(x-R)|^2$  looks as if  $R$  coincide with a maximum of the potential. Note that the result of the figure presents an intermediate regime where neither the adiabatic nor the diabatic approximations can be considered;  $g = 0.1$  and  $\Delta = 0.3$ .

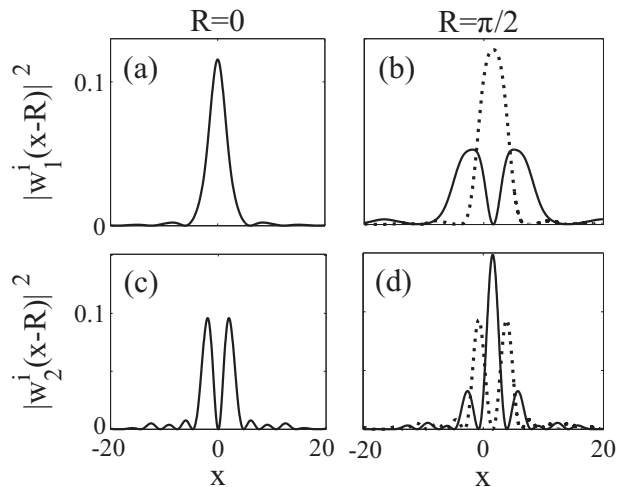


FIG. 2: The constituent squared amplitudes of the Wannier functions of the first, (a) and (b), and second, (c) and (d), Bloch band. The left plots display the Wannier functions for  $R = 0$ , while the right plots  $R = \pi/2$ , corresponding to the minima of  $V_{-}^{ad,d}(x)$  and  $V_{+}^{ad}(x)$  respectively. Solid lines depict  $|w_1^{+}(x-R)|^2$  and dashed line  $|w_1^{-}(x-R)|^2$ . The other dimensionless parameters are  $g = 0.1$  and  $\Delta = 0.25$ .

## B. Zero temperature many-body ground state

We will focus on the lowest band,  $\nu = 1$ , thus assuming a *filling factor*  $\xi = \frac{N}{K} < 1$ , where  $N$  is the total number of atoms and  $K$  number of sites. In the numerics  $K$  will be taken large enough (typically  $K > 100$ ) to assure small boundary effects. The  $N$  many-body ground states for fermions and bosons, at zero temperature and for filling factors  $\xi < 1$ , are

$$|\Psi\rangle_F = \prod_{q \in \mathcal{Q}} \hat{f}_q^{\dagger} |0\rangle = \prod_{q \in \mathcal{Q}} |n_q\rangle, \quad (20)$$

$$|\Psi\rangle_B = |n_0, n_{+1}\rangle, \quad n_0 + n_{+1} = N \quad (21)$$

respectively and  $\mathcal{Q}$  contains those values of  $q$  which are inside the Fermi sea,  $\hat{f}_q^{\dagger}$  is the Fermi creation operator of mode  $q$  of the lowest Bloch band,  $|0\rangle$  is the vacuum and  $n_q (= \langle \hat{n}_q \rangle)$  again characterizes the number of atoms in quasi momentum mode  $q$ ;  $\sum_{q \in \mathcal{Q}} n_q = N$ . Note that for bosons, the ground state is degenerate and  $n_0$  and  $n_{+1}$  may pertain any positive values such that the total number gives  $N$  (we have not included  $q = -1$  as it lies outside the Brillouin zone), and in fact any linear combination of these degenerate states is adequate. Further, the state (21) is valid for any filling factors  $\xi$ . The lowest Bloch band has maxima at  $q = \pm 1/2$  and minima at  $q = 0, +1$ . Consequently, for large lattices and a filling factor  $\xi < 1$  will the ground state form a type of atomic Schrödinger cat state, regardless of atomic type. In fact, the same holds in general for any non-integer filling factor

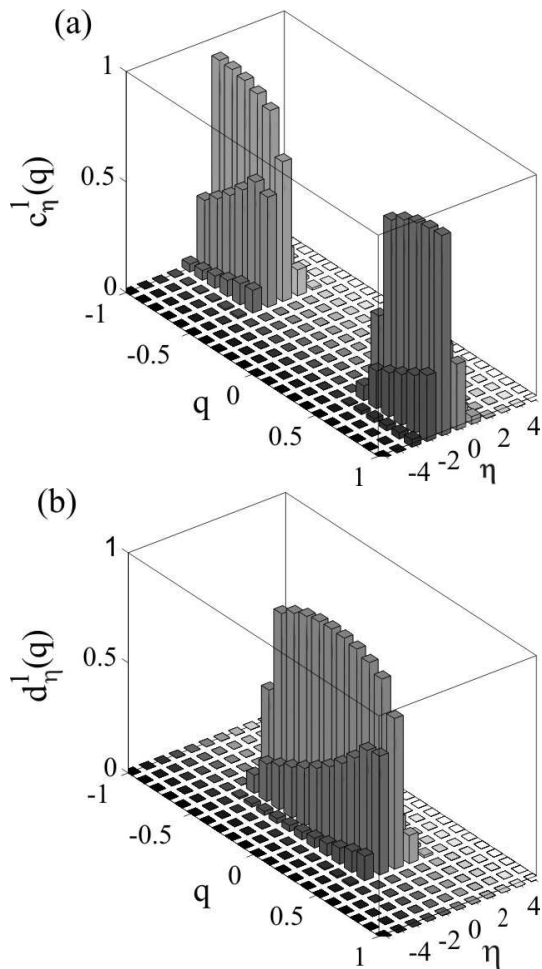


FIG. 3: Coefficients  $c_\eta^1(q)$  (a) and  $d_\eta^1(q)$  (b) defined in Eq. (11). The parameters are as in Fig. 1 (b), but with a larger coupling  $g = 0.5$ .

$\xi$ . As product states (20) and (21), there exist no correlation between the atoms. Nonetheless, entanglement between atomic motion and internal atomic states occurs for each atom (provided  $\Delta, g \neq 0$ ), which is clear since

$$\langle x|\psi_\nu(q)\rangle \neq \chi(x) (a|+\rangle + b|-\rangle), \quad (22)$$

for some normalized function  $\chi(x)$  and  $|a|^2 + |b|^2 = 1$ . The expansion of the Bloch eigenstates in terms of bare states is given in Eq. (11). The corresponding coefficients are displayed in Fig. 3, for the lowest Bloch band with parameters  $g = 0.5$  and  $\Delta = 0.25$ . For  $|q| < 1/2$ , the  $c_\mu^1(q)$  are all zero, while  $d_\mu^1(q) = 0$  for  $1/2 < |q| < 1$ . A result deriving from the block structure of the Hamiltonian (6). The  $c_\mu^1(q)$  coefficients are dominated by the ones with either  $\mu = 1$  or  $\mu = -1$ , and  $\mu = 0$  is the most prominent coefficient of the  $d_\mu^1(q)$ . Note that the probability for the atom to be found in the state  $|-\rangle$  for a given eigenstate  $\psi_\nu(q)$  is

$$P(-; \psi_\nu(q)) = \sum_{\eta \text{ even}} |c_\eta^\nu(q)|^2 + \sum_{\eta \text{ odd}} |d_\eta^\nu(q)|^2 \quad (23)$$

and  $P(+; \psi_\nu(q)) = 1 - P(-; \psi_\nu(q))$ .

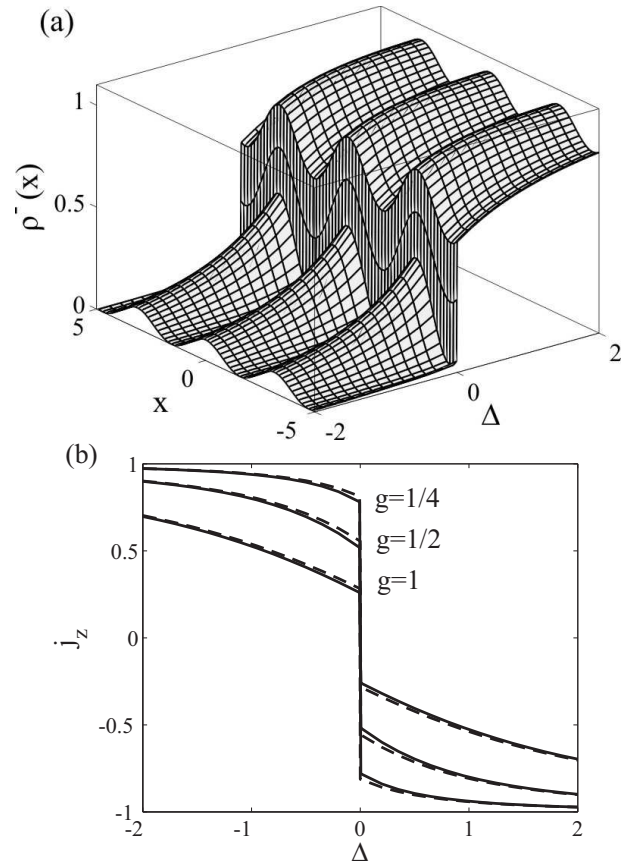


FIG. 4: The upper plot (a) displays the Fermi particle density  $\rho^-(x)$  (24) for the internal state  $|-\rangle$  at half filling of the lowest Bloch band. The lower plot (b) shows three examples of the collective atomic inversion  $j_z$  (25) as function of  $\Delta$  for bosons (dashed lines) and for fermions (solid lines). In (a)  $g = 1$ .

We define the internal density per particle as

$$\rho^\pm(x) = \frac{1}{N} \sum_\nu \sum_{q \in \mathcal{Q}} |\psi_{\nu,q}^\pm(x)|^2, \quad (24)$$

where the second sum runs over occupied momentum states, and  $N$  is the number of atoms. The density  $\rho^-(x)$  for fermions is shown in Fig. 4 (a) as function of the detuning  $\Delta$  where the lowest Bloch band is half filled,  $\xi = 1/2$ . For other filling factors one regains very similar plots. By substituting  $\Delta \leftrightarrow -\Delta$ , the  $\rho^+(x)$  is identical to  $\rho^-(x)$ . Noticeable is the discontinuity at  $\Delta = 0$ . Thus, around resonance,  $\Delta = 0$ , the population of  $|+\rangle$  and  $|-\rangle$  atoms may fluctuate and in particular a first order PT in the *collective atomic inversion* (per particle)

$$j_z \equiv \frac{1}{N} \sum_\nu \sum_{\{n_q\}} [P(+; \psi_\nu(q)) - P(-; \psi_\nu(q))] \quad (25)$$

is expected. Note that the above inversion (25) may be derived from the expectation value of the collective in-

version  $\hat{J}_z$

$$j_z = \frac{\langle \hat{J}_z \rangle}{N} \equiv \frac{1}{N} \sum_{i=1}^N \langle \hat{\sigma}_z^{(i)} \rangle, \quad (26)$$

where  $\hat{\sigma}_z^{(i)}$  is the  $i$ 'th atoms  $z$  Pauli matrix measuring the  $i$ 'th particle inversion. In the *Dicke model* of  $N$  two-level atoms interacting with a quantized field mode,  $j_z$  is often considered as an order parameter having a discontinuous first order derivative at the critical atom-field coupling which defines the *normal-superradiant quantum PT* [25]. The inversion  $j_z$  as function of  $\Delta$ , presented in Fig. 4 (b), illustrates the discontinuity incorporated in our model. Note that this PT is different from the one of the Dicke model. We have verified that the same kind of phenomenon is obtained also when one restricts the dynamics to one of the subsets (6). Assuming a single particle in either of the subsets (6), one has  $E_1(\pm 1) = E_1(0)$  for  $\Delta = 0$ , while  $E_1(\pm 1) \neq E_1(0)$  for  $\Delta \neq 0$  (clear for example from the dashed curve in Fig. 1). Note that this is not true if we include both subsets where  $E_1(\pm 1) = E_1(0)$  is always true (here  $E_1(q)$  is the lowest Bloch band of either  $H_\phi$  or  $H_\varphi$ ). Thus, the single particle ground state energy is either  $E_1(\pm 1)$  or  $E_1(0)$  depending on the sign of  $\Delta$ , and as one tunes  $\Delta$  across resonance the atom will absorb/emitt one photon and  $W \rightarrow -W$ . The same argument holds also for many atoms where each one of them swaps internal states,  $|\pm\rangle \leftrightarrow |\mp\rangle$ , while passing through  $\Delta = 0$ . The PT is of topological character, since, in Fermionic systems, the structure of the Fermi surface changes across the critical point. Topological PTs, or Lifshitz transition, have been studied comprehensively in quantum Hall and superconducting systems [14, 15]. However, a recent paper considered a topological PT of ultracold fermionic atoms in an anisotropic three dimensional optical lattice [16].

### C. Non-zero temperature ground state

We turn now to the situation of non-zero temperature and thermal excitations. As argued above, each eigenstate  $|\psi_1(q)\rangle$  in the zero temperature ground state undergoes a collective Rabi flip by sweeping the detuning across resonance, which suggests that also for excitations around the Fermi surface or of the Boson ground state will the atomic inversion be discontinuous around  $\Delta = 0$ . Let us introduce the gap function

$$\delta j_z = \lim_{\Delta \rightarrow 0^-} j_z - \lim_{\Delta \rightarrow 0^+} j_z \quad (27)$$

and study the behavior of  $\delta j_z$  for various temperatures  $T$ . The temperature dependence of the collective atomic inversion  $j_z$  and the inversion gap  $\delta j_z$  is presented in Figs. 5 (a) and (b) respectively. The gap is slightly larger for Bosons than for Fermions. Surprisingly, the gap  $\delta j_z$  approaches a non-zero value ( $\approx 0.75$  for this choice of coupling;  $g = 1/2$ ) in the large temperature limit. Even

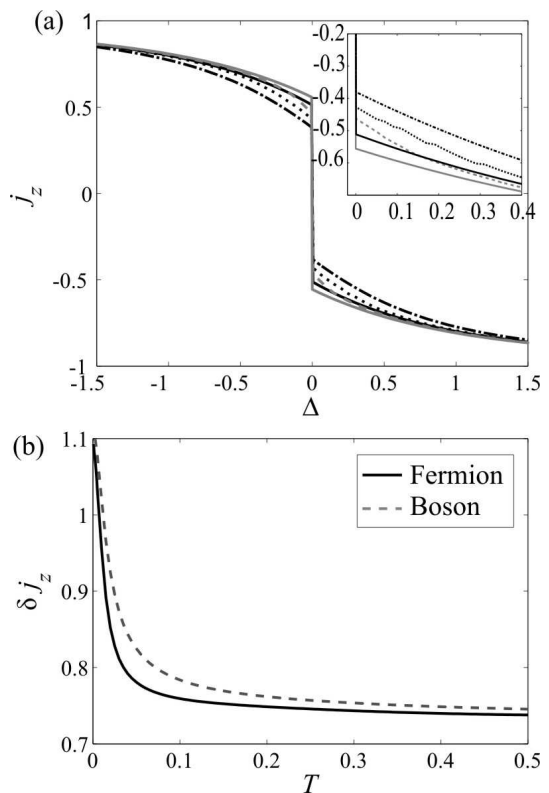


FIG. 5: The collective atomic inversion  $j_z$  (a) for fermions (black lines) and bosons (gray lines) as function of the detuning  $\Delta$  and different temperatures, fermions:  $T = 0$  (solid line),  $T = 0.02$  (dotted) and  $T = 0.1$  (dot-dashed) and bosons:  $T = 0$  (solid line) and  $T = 0.1$  (dashed line). The inset is a close-up of the curves to the right of  $\Delta = 0$ . The second figure (b) depicts the temperature dependence of the inversion gap  $\delta j_z$  of Eq. 27, for Fermions (solid black line) and bosons (dashed gray line). In both plots,  $g = 1/2$  and the chemical potential is chosen such that the number of particles is half the lattice number.

at fairly large couplings, this asymptotic value is non-zero.

Another question of relevance is the amount of populations of excited quasi momentum states  $|\psi_\nu(q)\rangle$  for non-zero temperatures, especially for fermions. The two lowest Bloch bands are identical at resonance,  $\Delta = 0$ , and consequently equally populated. For small temperatures, only states corresponding to these two bands are substantially occupied, while for large temperatures also the third and fourth band will be populated. For non-zero detuning, the degeneracy is lifted and the populations of the two lowest bands are no longer balanced. We may define the individual band population

$$P_\nu = \sum_{q \in (-1,1]} \langle \hat{n}_q^\nu \rangle, \quad (28)$$

where  $\langle \hat{n}_q^\nu \rangle = \text{Tr} [\rho_T \hat{n}_q^\nu]$  is the expectation value of the number operator  $\hat{n}_q^\nu$  for the state  $\rho_T$  given at temperature



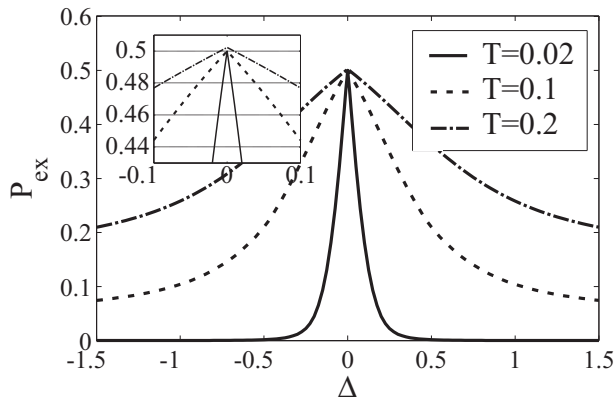


FIG. 6: Population of excited bands  $P_{ex}$ , in the case of fermions, as function of the detuning and of temperature;  $T = 0.02$  (solid line),  $T = 0.1$  (dashed line) and  $T = 0.2$  (dot-dashed line). At resonance and moderate temperatures, the excited population approximates  $1/2$  due to the degeneracy at that point. For large detuning, the gap between the two lowest bands increases causing a decrease in the excited band population. The inset shows a close-up of the population around  $\Delta = 0$ , indicating that for large temperatures  $P_{ex}$  exceeds  $1/2$  at resonance due to occupation of third and higher bands. Here  $g = 1/2$  and  $\xi = 1/2$ .

$T$ . Thus,  $P_\nu$  measures the population in band  $\nu$ , and in particular for  $\Delta = 0$  do we have  $P_i = P_{i+1}$  for  $i = 1, 2, 3, \dots$  due to the degeneracy. The total population of excited bands is given by

$$P_{ex} = \sum_{\nu=2}^{\infty} P_\nu. \quad (29)$$

Note that  $P_{ex}$  includes the second band  $\nu = 2$  which for  $\Delta = 0$  is degenerate with the lowest band  $\nu = 1$  and in this special case is the subscript  $ex$  (excited) misleading. Naturally,  $0 \leq P_{ex} < 1$  and also  $1/2 \leq P_{ex}(\Delta = 0) < 1$ . Figure 6 displays  $P_{ex}$  as function of  $\Delta$  and for three different temperatures. Expectedly, the excitations increase for a large temperature and decrease for a large detuning. The inset gives the population close to resonance, and it is in particular seen that  $P_{ex}(\Delta = 0) > 1/2$  ( $P_{ex}(\Delta = 0) = 0.5025$  for  $T = 0.2$ ) from the fact that the bands  $\nu = 3, 4, \dots$  begin to be populated. The shape of  $P_{ex}$  seems fairly Lorentzian, but the inset reveals that  $P_{ex}$  is indeed not Lorentzian in the vicinity of  $\Delta = 0$ . Again we restrict the analysis to a filling factor  $\xi = 1/2$ , namely chose the chemical potential  $\mu$  such that it results in half filling.

#### D. Extension to a higher dimensional optical lattice

We conclude this section by discussing the situation of a two dimensional optical lattice. The two fields is assumed to share the same wavelength  $\lambda$  and both interact with the same dipole transition of the atom. The

Hamiltonian takes the form

$$\hat{H}_{2D} = -\frac{\partial^2}{\partial x^2} + \begin{bmatrix} \frac{\Delta}{2} & 2g_x \cos(\hat{x}) + 2g_y \cos(\hat{y}) \\ 2g_x \cos(\hat{x}) + 2g_y \cos(\hat{y}) & \frac{\Delta}{2} \end{bmatrix}. \quad (30)$$

The lowest energy band in the symmetrical case with  $g_x = g_y = 0.1$  and  $\Delta = 0.25$  is shown in Fig. 5. As for the one dimensional case, for  $q_x, q_y = \pm 1/2$  the lowest energy band attains its maximum. Importantly, multiple minima of the dispersion is also found in the two dimensional case. It is easy to convince oneself that this holds also in three dimensional, and consequently that the topological PT is not limited to the one dimensional lattice.

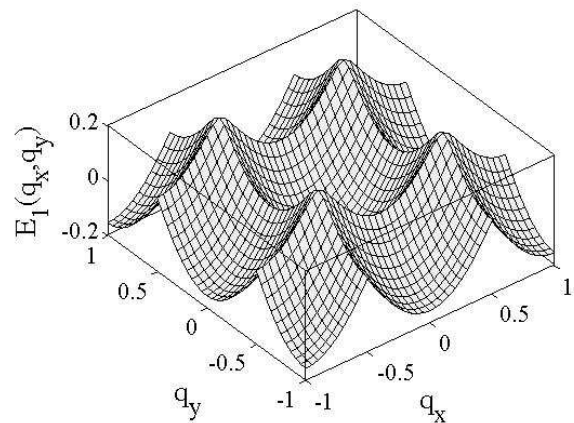


FIG. 7: First energy band  $E_1(q_x, q_y)$  of the two dimensional model (30), with equal coupling strengths  $g_x = g_y = 0.1$  and  $\Delta = 0.25$ .

## IV. CONCLUSIONS

In this paper have we studied an ideal gas of ultra-cold two-level atoms coupled to an optical lattice. It was shown that the coupled two-level character of the problem give rise to novel phenomena, not present in the regular dispersive case of large detuning where one atomic level has been adiabatically eliminated rendering an internal structureless system. In particular, the Brillouin zone is twice as large in this system compared to a internal structureless one and the Bloch bands possess multiple minima. This comes about due to the competition between the various involved terms of the Hamiltonian; kinetic and internal energy. An outcome of the peculiar energy band spectrum is the presence of a topological, or Lifshitz, PT as the detuning is tuned across resonance. This transition is of first order nature and is manifested

in the collective atomic inversion. Moreover, it was found to be a non-zero temperature PT.

To conclude, we showed that quantum PTs can occur in multi-component ultracold atomic systems despite the lack of atom-atom interaction. It is believed that adding scattering between atoms will yield a rich phase diagram with possible new types of phases, which we are currently investigating. We further plan to analyze the current system, and especially the topological PT, in a cavity QED model where the field is treated quantum mechanically.

## APPENDIX A: EFFECTIVE DISIPATIONLESS TWO-LEVEL MODEL

Decay of the excited atomic level will typically set limits on any experimental consideration. One way to minimize such effects is to effectively couple two metastable atomic states using an additional laser. We consider therefore a three-level  $\Lambda$ -atom with metastable lower states  $|1\rangle$  and  $|2\rangle$  and excited state  $|3\rangle$ , with respective energies  $E_i$ ,  $i = 1, 2, 3$ . State 1 and 3 are coupled through our optical lattice, while 2 and 3 couple via an external laser whose field amplitude is assumed constant over the atomic sample. The Hamiltonian becomes [26]

$$\hat{H}_\Lambda = \sum_{i=1}^3 E_i \hat{\sigma}_{ii} + \Omega (\hat{\sigma}_{23} e^{i\omega_L t} + \hat{\sigma}_{32} e^{-i\omega_L t}) + 2g \cos(\hat{x} + \omega_O t) (\hat{\sigma}_{13} + \hat{\sigma}_{31}), \quad (\text{A1})$$

where  $\Omega$  is the external laser coupling amplitude,  $\omega_L$  and  $\omega_O$  the two field frequencies, and  $\hat{\sigma}_{ij} = |i\rangle\langle j|$ . The excited state can be adiabatically eliminated if the interaction is dispersive. Thus, we assume a highly detuned configuration,  $\Delta_1 = E_{33} - E_{22} - \omega_L \gg \Omega$  and  $\Delta_2 = E_{33} - E_{11} - \omega_O \gg 2g$ , and at the same time  $\Delta_3 = |\Delta_1 - \Delta_2|$  is of the same order as  $\Omega$  and  $g$ . One then derives, after application of a rotating wave approximation, an effective two-level model for the metastable states, which is given by [26]

$$\hat{H}_{eff} = \frac{\Delta_3}{2} \hat{\sigma}_z - \frac{\Omega^2}{\Delta_1} \hat{\sigma}_{22} + \frac{4g^2}{\Delta_2} \cos^2(\hat{x}) \hat{\sigma}_{11} + 2g\Omega \cos(\hat{x}) \left( \frac{1}{\Delta_1} + \frac{1}{\Delta_2} \right) \hat{\sigma}_x, \quad (\text{A2})$$

where  $\hat{\sigma}_z = |2\rangle\langle 2| - |1\rangle\langle 1|$  and  $\hat{\sigma}_x = |1\rangle\langle 2| + |2\rangle\langle 1|$ . We have numerically confirmed that the band structure of (A2) looks very similar to the ones presented in Fig. 1. Therefore our results and conclusions of Sec. III are also reproducible for a Hamiltonian such as (A2).

## II. ACKNOWLEDGEMENTS

We wish to thank Prof. Maciej Lewenstein and Dr. Giovanna Morigi for inspiring discussions.

- 
- [1] D. Jaksch, C. Bruder, J. I. Cirac, C. W. Gardiner, and P. Zoller, *Phys. Rev. Lett.* **81**, 3108 (1998).
- [2] M. Greiner, O. Mandel, T. Esslinger, T. W. Hänsch, and I. Bloch, *Nature* **415**, 39 (2002).
- [3] M. Lewenstein, A. Sanpera, V. Ahufinger, B. Damski, A. Sen, and U. Sen, *Adv. Phys.* **56**, 243 (2007).
- [4] B. Damski, J. Zakrzewski, L. Santos, P. Zoller, and M. Lewenstein, *Phys. Rev. Lett.* **91**, 080403 (2003); U. Gavish, and Y. Castin, *Phys. Rev. Lett.* **95**, 020401 (2005); B. Juliette, V. Josse, Z. Zuo, A. Bernard, B. Hambrecht, P. Lugan, D. Clément, L. Sanchez-Palencia, P. Bouyer, and A. Aspect, arXiv:0804.1621; G. Roati, C. D'Errico, L. Fallani, M. Fattori, C. Fort, M. Zaccanti, G. Modugno, and M. Inguscio, arXiv:0804.2609.
- [5] L. Santos, M. A. Baranov, J. I. Cirac, H. U. Everts, H. Fehrmann, and M. Lewenstein, *Phys. Rev. Lett.* **93**, 030601 (2004); S. Wessel, and M. Troyer, *Phys. Rev. Lett.* **95**, 127205 (2005);
- [6] B. Parades, A. Widera, V. Murg, O. Mandel, S. Fölling, I. Cirac, G. V. Schlyapnikov, T. W. Hänsch, and I. Bloch, *Nature* **429**, 277 (2004).
- [7] A. S. Sørensen, S. Demler, and M. D. Lukin, *Phys. Rev. Lett.* **94**, 086803 (2005); R. N. Palmer, and D. Jaksch, *Phys. Rev. Lett.* **96**, 180407 (2007).
- [8] R. Raussendorf, and H. J. Briegel, *Phys. Rev. Lett.* **86**, 5188 (2001); I. H. Deutsch, G. K. Brennen, and P. S. Jessen, *Fort. Phys.- Prog. Phys.* **48**, 925 (2000).
- [9] E. Demler, and F. Zhou, *Phys. Rev. Lett.* **88**, 163001 (2002); A. Imambekov, M. Lukin, and E. Demler, *Phys. Rev. A* **68**, 063602 (2003); F. Zhou and M. Snoek, *Ann. Phys.* **3008**, 692 (2003); J. J. Garcia-Ripoll, M. A. Martin-Delgado, and J. I. Cirac, *Phys. Rev. Lett.* **93**, 250405 (2005); T. Kimura, S. Tsuchiya, and S. Kurihara, *Phys. Rev. Lett.* **94**, 110403 (2005); R. V. Pai, K. Sheshadri, and R. Pandit, *Phys. Rev. B* **77**, 014503 (2008).
- [10] A. Albus, A. Alluminati, and J. Eisert, *Phys. Rev. A* **68**, 023606 (2003); H. P. Buchler, and G. Blatter, *Phys. Rev. Lett.* **91**, 130404 (2003); M. Lewenstein, L. Santos, M. A. Baranov, and H. Fehrmann, *Phys. Rev. Lett.* **92**, 050401 (2004); K. Gunter, T. Stoferle, H. Moritz, M. Kohl, and T. Esslinger, *Phys. Rev. Lett.* **96**, 180402 (2006).
- [11] S. Sachdev, *Quantum Phase Transitions*, (Cambridge University Press, 2006).
- [12] K. V. Kuritsky and R. Graham, *Phys. Rev. Lett.* **91**, 240406 (2003).
- [13] K. V. Kuritsky and R. Graham, *Phys. Rev. A* **70**, 063610 (2004); K. V. Kuritsky, M. Timmer, and R. Graham, *Phys. Rev. A* **71**, 033623 (2005).
- [14] G. E. Volovik, in *Quantum Analogues: From Phase Transition to Black Holes and Cosmology*, pages 31-73 (Springer-Verlag, 2007), arXiv: cond-mat/0505089.
- [15] M. J. P. Ginigras and D. A. Huse, *Phys. Rev. B* **53**, 15193 (1996); B. A. Bernevig, T. L. Hughes and S. C. Zhang, *Science* **314**, 1757 (2006); H. Watanabe and M. Ogata, *Phys. Rev. Lett.* **99**, 136401 (2007); N. Doiron-Leyraud, C. Proust, D. Lebof, J. Levallois, J. B. Bonnemaïson,



- R. X. Liang, D. A. Bonn, W. N. Hardy and L. Taillefer, *Nature* **447**, 565 (2007).
- [16] R. W. Cherng and C. A. R. Sá de Melo, arXiv:0808.1426.
- [17] *Handbook of mathematical Functions*, Natl. Bur. Stand. Appl. Math. Ser. No. 55, edited by M. Abramowitz and I. A. Stegun (U.S. GPO, Washington, D.C., 1972).
- [18] D. Wang, T. Hansson, Å. Larson, H. O. Karlsson, and J. Larson, *Phys. Rev. A* **77**, 053808 (2008).
- [19] W. Ren and H. J. Carmichael, *Phys. Rev. A* **51**, 752 (1995).
- [20] J. Larson, J. Salo, and S. Stenholm, *Phys. Rev. A* **72**, 013814 (2005).
- [21] J. Larson and S. Stenholm, *Phys. Rev. A* **73**, 033805 (2006).
- [22] A. S. Davydov, *Quantum Mechanics*, 2nd ed. (Pergamon, Oxford, 1976).
- [23] J. Larson, *Phys. Rev. A* **73**, 013823 (2006).
- [24] N. W. Ashcraft and D. Mermin *Solid State Physics*, (Fortworth Tx, Harcourt Brace Collage Publishers, 1976).
- [25] Y. K. Wang and F. T. Hioe, *Phys. Rev. A* **7**, 831 (1973); K. Hepp and E. H. Lieb, *Ann. Phys.* **76**, 360 (1973); C. Emary and T. Brandes, *Phys. Rev. Lett.* **90**, 044101 (2003); F. Dimer, B. Estienne, A. S. Parkins, and H. J. Carmichael, *Phys. Rev. A* **75**, 013804 (2007).
- [26] M. Alexanian and S. K. Bose, *Phys. Rev. A* **52**, 2218 (1995).